



Characterization of cobalt oxides studied by FT-IR, Raman, TPR and TG-MS

Chih-Wei Tang^a, Chen-Bin Wang^{b,*}, Shu-Hua Chien^{c,d,**}

^a Department of Chemistry, Chinese Military Academy, Kaohsiung 83059, Taiwan, ROC

^b Department of Applied Chemistry and Materials Science, Chung Cheng Institute of Technology, National Defense University, Tahsi, Taoyuan 33509, Taiwan, ROC

^c Institute of Chemistry, Academia Sinica, Taipei 11529, Taiwan, ROC

^d Department of Chemistry, National Taiwan University, Taipei 10764, Taiwan, ROC

ARTICLE INFO

Article history:

Received 20 February 2008

Received in revised form 22 April 2008

Accepted 23 April 2008

Available online 29 April 2008

Keywords:

Cobalt oxides

Thermal analysis

TG-MS

ABSTRACT

The as-prepared cobalt oxide (assigned as CoO_x) was fabricated by precipitation–oxidation from aqueous cobalt nitrate solution using sodium hydroxide and oxidation with hydrogen peroxide. Another series of pure cobalt oxides was refined by the decomposition of CoO_x in a nitrogen environment at temperatures of 280, 450 and 950 °C (D-280, D-450 and D-950, respectively). Phase transformation, structural properties and red-ox properties were characterized by thermogravimetry-mass spectrometry (TG-MS), X-ray diffraction (XRD), infrared spectroscopy (IR), Raman spectroscopy and temperature-programmed decomposition/reduction (TPD/TPR). Analysis of the thermal behavior on CoO_x revealed that a series of pure cobalt oxide with particle sizes of 10–20 nm could be obtained easily. The results demonstrated that the refined samples D-280, D-450 and D-950 were $\text{CoO}(\text{OH})$, Co_3O_4 and CoO , respectively.

© 2008 Elsevier B.V. All rights reserved.

1. Introduction

Cobalt oxide has a wide range of applications in various industrial sectors, including in rechargeable batteries [1], as a catalyst of the abatement of CO [2], as a magnetic material [3] and in CO sensors [4]. Five species of cobalt oxide [CoO_2 , Co_2O_3 , $\text{CoO}(\text{OH})$, Co_3O_4 and CoO] have been reported [4–9]. However, cobalt oxide with a valence of more than three is unstable in the natural environment. Other cobalt oxides [Co_3O_4 and CoO] are more stable and useful in industry. Cobalt oxyhydroxide, $\text{CoO}(\text{OH})$, has a hexagonal structure in which a divalent metal cation is located at an octahedral site which is coordinated by six hydroxyl oxygen. Well-spread $\text{CoO}(\text{OH})$ can be used as the conductive network in rechargeable alkaline batteries [5]. CoO is an antiferromagnetic material whose magnetic characteristics [10,11] and application of gas-sensors [12,13] have been extensively studied. CoO nanocomposite film in gas-sensing. Co_3O_4 exhibited high catalytic activity in CO oxidation [14–16]. The spinel trivalent cobalt tetraoxide, Co_3O_4 , has an energy band-gap of 1.4–1.8 eV [17] that can be used as a p-type semiconductor and an antiferromagnetic material [18,19]. The distribution of cations on spinel Co_3O_4 is shown to be $\text{Co}^{2+}[\text{Co}_2^{3+}] \text{O}_4^{2-}$: the cations inside parentheses are octahedral and those outside are tetrahe-

drally coordinated with oxygen ions. The complex is stable up to 800 °C and decomposes to CoO [14,20,21] above 900 °C.

A preview paper [9] reported that variation in the morphology of cobalt oxides with calcination and reduction pretreatments. Figlarz et al. found that the hexagonal Co_3O_4 was obtained by the decomposition of $\text{CoO}(\text{OH})$ at approximately 250 °C, based on analysis by X-ray diffraction (XRD) and selected-area electron diffraction (SAED). To understand the phase transformation and the composition of decomposed outlet gases, this work discusses the analysis of the thermogravimetry-mass spectrometry (TG-MS). Temperature-programmed decomposition (TPD), X-ray diffraction (XRD), infrared spectroscopy (IR), Raman spectroscopy and temperature-programmed reduction (TPR) are employed to characterize a series of cobalt oxides.

2. Experimental

2.1. Preparation of cobalt oxides

The as-prepared cobalt oxide (assigned as CoO_x) with a high valence state of cobalt was synthesized by the precipitation–oxidation method in an aqueous solution. The precipitation process was carried out at 50 °C with 50 ml of 0.6 M $\text{Co}(\text{NO}_3)_2 \cdot \text{H}_2\text{O}$ solution added drop by drop to 100 ml of 3.2 M NaOH solution; 100 ml of H_2O_2 (50 wt%) was then introduced dropwisely under constant stirring. In order to avoid the contamination of chloride ion, the H_2O_2 was chosen as an oxidizing agent instead of NaOCl [22]. The precipitate was then filtered, washed with deionized water and dried in

* Corresponding author.

** Corresponding author at: Institute of Chemistry, Academia Sinica, Taipei 11529, Taiwan, ROC.

E-mail addresses: chenbinwang@gmail.com (C.-B. Wang), chiensh@gate.sinica.edu.tw (S.-H. Chien).

an oven at 110 °C for 24 h. The dried CoO_x was ground and preserved in a desiccator as fresh samples. Further, other series of pure cobalt oxide were refined from the decomposition of CoO_x under nitrogen environment at different temperatures: 280, 450 and 950 °C, respectively (assigned as D-280, D-450 and D-950, respectively).

2.2. Characterization techniques

X-ray diffraction (XRD) measurements were performed using a Siemens D5000 diffractometer with Cu Kα1 radiation ($\lambda = 1.5405 \text{ \AA}$) at 40 kV and 30 mA with a scanning speed in 2θ of 2° min^{-1} . Using the XRD diffraction data, the crystallite sizes of cobalt oxides were able to be estimated using the Scherrer equation.

$$d = \frac{0.9\lambda}{B \cos \theta_B} \quad (1)$$

In this equation, d is the crystallite size (nm); λ the X-ray wavelength; B the full width at half maximum of the diffraction peak at θ_B ; θ_B is the diffraction angle.

Specific surface area measurements were carried out by using the Brunauer–Emmett–Teller (BET) method on a Micromeritics ASAP 2010 apparatus. Nitrogen adsorption isotherms at -196°C were determined volumetrically. The catalysts were pre-outgassed at 5×10^{-5} Torr for 3 h at 110 °C. The surface area was determined from the nitrogen adsorption isotherm.

IR spectra of samples were obtained by a Bomem DA-8 spectrometer with a resolution of 4 cm^{-1} in the range of $450\text{--}1000 \text{ cm}^{-1}$. One milligram of each powder sample was diluted with 200 mg of vacuum-dried IR-grade KBr powder and subjected to a pressure of 10 tons. The measurements of Raman spectroscopy were recorded using a Nicolet Almega XR dispersive Raman spectrometer. The spectra were collected between 300 and 900 cm^{-1} , using a beam of diode laser (780 nm), with the sample exposed to the air under ambient conditions.

TPR of a series of cobalt oxides was performed using 10% H₂ in Ar as the reducing gas. The flow rate of H₂/Ar was adjusted by mass flow controller under 25 ml min^{-1} . The cell was a quartz tube with an inner diameter 8 mm and 80 mg of the catalyst was mounted with quartz wool. The hydrogen consumption was monitored by a thermal conductivity detector (TCD) on raising the sample temperature from RT to 500 °C at a constant rate of 5°C min^{-1} . TPD profile of CoO_x sample was performed using He as carrier gas. The flow rate of He was adjusted to 25 ml min^{-1} . The oxygen desorption was monitored by a TCD on raising the sample temperature from RT to 1000 °C at a constant rate of $10^\circ\text{C min}^{-1}$.

On-line TG-MS analyses of the gases evolved from the sample were performed simultaneously using the STA-409CD with Skimmer coupled to a quadruple mass spectrometer QMA 400 (maximum 512 amu). The TG experiments were operated from RT to 1100 °C with heating rate of $10^\circ\text{C min}^{-1}$ under a continuous flow of He (100 ml min^{-1}). A transfer line, specially designed to connect a vacuum pump in order to optimize the amount of evolved gas, transferred from the TG to the MS. A mass analysis was performed each 2 s recording mass fragments between 2 and 300 atomic mass

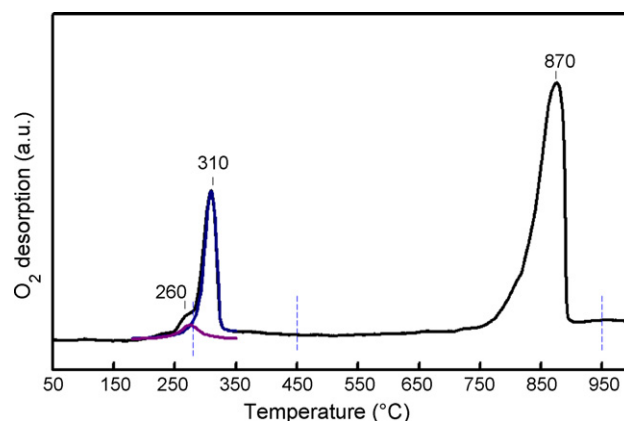


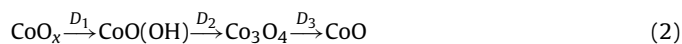
Fig. 1. TPD profile of CoO_x.

units (amu). The measurement of outlet gas via mass spectrometric intensities was plotted as a function of temperature that showed two well separated regions of de-volatilization.

3. Results and discussion

3.1. Structural analysis of cobalt oxides

Fig. 1 displays the TPD profile of the as-prepared CoO_x sample. Three peaks of oxygen desorption at different temperatures (T_d) – D_1 ($T_d = 260^\circ\text{C}$), D_2 ($T_d = 310^\circ\text{C}$) and D_3 ($T_d = 870^\circ\text{C}$) – are observed. The sequential desorption of oxygen from CoO_x indicates that cobalt oxide with different oxidation states may be obtained by the appropriate thermal decomposition of CoO_x in a nitrogen environment.



Cobalt ions with an oxidation state of +3 [CoO(OH)], +8/3 [Co₃O₄] and +2 [CoO] may be obtained from CoO_x by thermal decomposition at 280, 450 and 950 °C, respectively. Samples prepared in this way are designated herein as D-280, D-450 and D-950. Although D_1 and D_2 peaks in the spectrum are merged together, the desired pure sample of CoO(OH) is easily obtained by the simple thermal decomposition of CoO_x at 280 °C in the TPD system (see the characterizations below).

Fig. 2 shows XRD patterns of refined species of cobalt oxide. Columns 2–4 of Table 1 presents the species, crystal phase and particle size of these oxides. The diffraction profile of the D-280 sample (Fig. 2(a)) matches the JCPDS (PDF-74-1057) [23] file, identifying cobalt oxyhydroxide, CoO(OH), with a hexagonal structure. The average particle size is small (10 nm, according to the peak width and the Scherrer equation). The D-450 sample (Fig. 2(b)) matches the JCPDS (PDF-76-1802) file identifying cobaltic oxide, Co₃O₄, with a spinel structure. The D-950 sample (Fig. 2(c)) matches the JCPDS (PDF-71-1178) file for cobaltous oxide, CoO, with a face-centered cubic (fcc) structure. The peak width in the D-950 pattern

Table 1

A series of the species of cobalt oxide for characterization

Samples	XRD		S_{BET}	FT-IR ($\text{m}^2 \text{ g}^{-1}$) $\nu_{\text{Co-O}}$ (cm^{-1})	Raman shift (cm^{-1})	TPR (C)		
	Structure ^a	d (nm) ^b				Co ₃ O ₄	CoO	Co
CoOOH	Hexagonal	10	59	584	367, 482, 599, 809	240	295	500
Co ₃ O ₄	Spinel	11	55	570, 661	482, 519, 621, 690	–	340	500
CoO	fcc	16	5	507	455, 675	–	–	550

^a According to the data base of JCPDS2001.

^b Particle size by Debye–Scherrer equation with CoOOH(1 1 1), Co₃O₄(3 1 1) and CoO(2 0 0) peak.

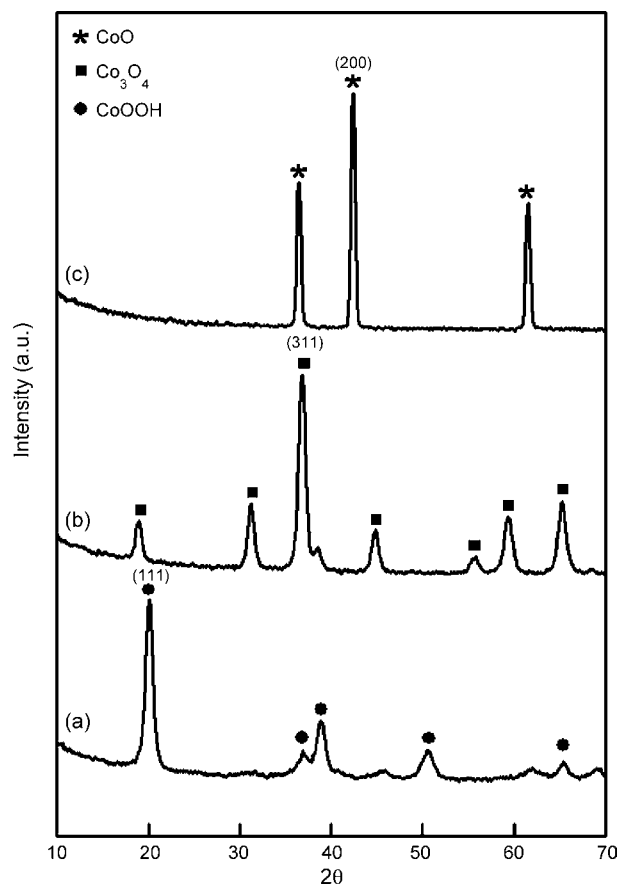


Fig. 2. XRD profiles of (a) D-280 (b) D-450 (c) D-950.

indicates substantial sintering of primary crystallites (d increases to 16 nm). Nitrogen adsorption isotherms on a series of cobalt oxides are obtained at -196°C . They are similar across the adsorbents of interest. They are type II by Brunauer's classification. The decrease in the surface area (column 5 in Table 1) is associated with the sintering of D-950 sample.

The phase transformation revealed by XRD is accompanied by simultaneous variation in both IR and Raman spectra. Fig. 3 shows the IR absorption spectra of D-280, D-450 and D-950 samples. The IR spectra of D-280 and D-950 samples (Fig. 3(a) and (c)) display single bands (584 and 507 cm^{-1}) that are likely to be associated with the cobalt ion in octahedral holes, meaning in an oxygen octahedral environment [24].

The variation may be caused by the difference between their structures (hexagonal vs. face-centered cubic). The IR spectrum of D-450 sample (Fig. 3(b)) displays two distinct bands that originate from the stretching vibrations of the metal-oxygen bonds [22,23,25]. The first band (ν_1) at 570 cm^{-1} is associated with the OB_3 vibration in the spinel lattice, where B denotes Co^{3+} in an octahedral hole. The second band (ν_2) at 661 cm^{-1} is attributed to the ABO_3 vibration, where A denotes the Co^{2+} in a tetrahedral hole.

Fig. 4 displays the Raman spectra of a series of the cobalt oxides formed by thermal decomposition. The D-280 sample has bands at 367 , 482 , 599 and 809 cm^{-1} (Fig. 4(a)), which are assigned to $\text{CoO}(\text{OH})$. Following the higher-temperature treatments, different bands were observed at 482 , 519 , 621 , 690 cm^{-1} for D-450 (Fig. 4(b)) and 455 , 675 cm^{-1} for D-950 (Fig. 4(c)), probably because of the phase transformation under heat treatment. The prominent Raman peaks correspond to the E_g (482 cm^{-1}), F_{2g} (519 and 621 cm^{-1}), A_{1g} (690 cm^{-1}) modes of the Co_3O_4 crystalline phase (D-450) and are

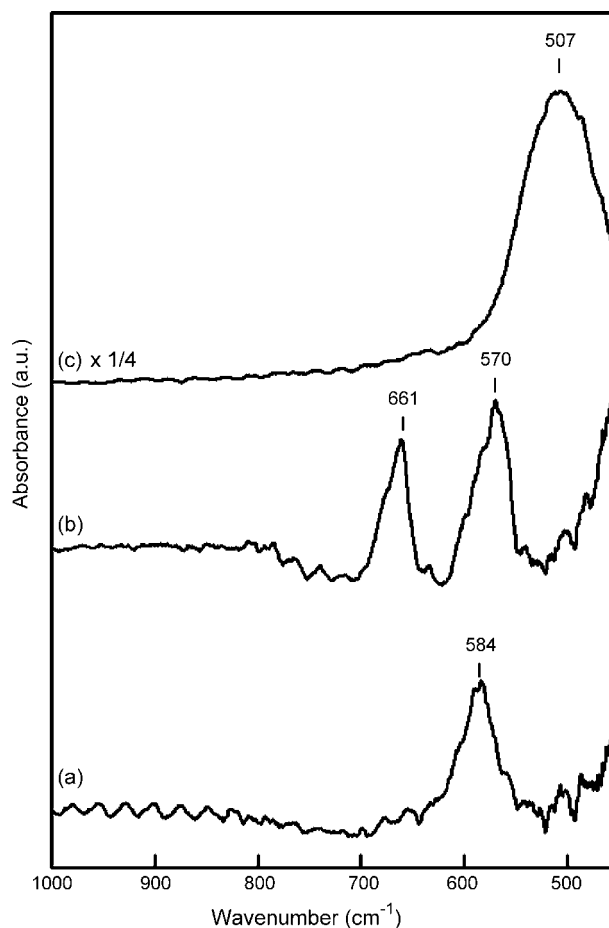


Fig. 3. FTIR spectra of (a) D-280 (b) D-450 (c) D-950.

consistent previous investigations [26,27]. Upon heat treatment at 950°C , the 519 and 621 cm^{-1} peak disappeared and broad bands at 455 and 675 cm^{-1} appeared, because of the formation of cubic CoO . These are shifted from the positions of the main peaks, 672 and 468 cm^{-1} , in previous studies of bulk CoO [28–30], shifted because of the nano-sized effect. This result confirms that the crystalline structure of the series of cobalt oxides can be identified by Raman spectroscopy.

3.2. Reductive behavior of cobalt oxides

Fig. 5 compares the reduction behavior of the series of cobalt oxides. The D-280 sample (Fig. 5(a)) yields three sequent signals at 215 , 260 and 350°C . According to our previous study [2], we have stopped each TPR step (under three reduction temperature) to record the XRD pattern of the sample and then to have a definitive knowledge of the phase formed after each reduction peak (from $\text{CoO}(\text{OH})$ to Co_3O_4 , then to CoO). So, we suggests that the $\text{CoO}(\text{OH})$ (D-280) is initially reduced to Co_3O_4 , and then further reduced to CoO and Co metal. The following equations are designated.

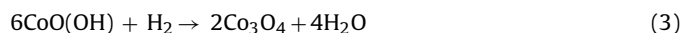


Fig. 5(b) shows the TPR profile of D-450 sample; it includes only two reductive singles at 300 and 367°C . Sexton et al. [31] found that the reduction profile of Co_3O_4 includes a low-temperature peak below 300°C and a high-temperature peak at approximately

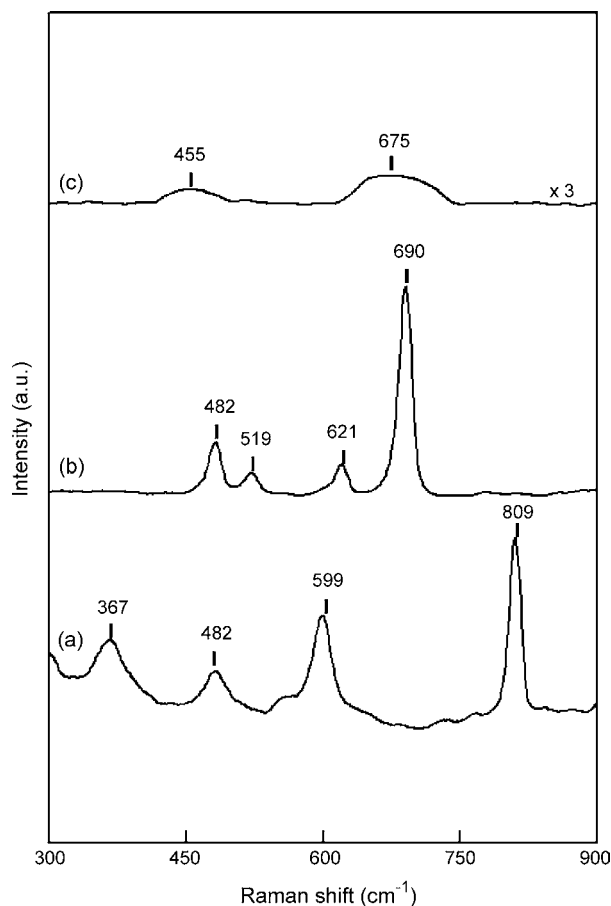


Fig. 4. Raman spectra of (a) D-280 (b) D-450 (c) D-950.

500 °C. According to the literature [32–35], the low-temperature peak is associated with the reduction of Co^{3+} ions to Co^{2+} (Eq. (4)) with the subsequent structural change to CoO. The second higher temperature peak is due to the reduction of CoO to metallic cobalt (Eq. (5)). A comparison with the D-280 sample, and in particular, the disappearance of the peak at around the lowest temperature indicates that the reductive behavior is in good agreement with the proposed Co_3O_4 . The TPR profile of the D-950 sample (Fig. 5(c)) includes only a single peak, which is assigned unambiguously to the direct reduction of CoO to cobalt metal.

3.3. Analysis of evolved gas of cobalt oxides

To confirm the phase transformation of $\text{CoO}(\text{OH})$ to Co_3O_4 and CoO under heat treatment, coupled quantitative and qualitative analysis by TG-MS was performed to prove the structural identifications in Section 3.1. Fig. 6 presents the TG-MS profile of the D-280 sample. The thermogravimetric plot presents two marked weight losses at about 280 and 850 °C. Column 4 in Table 2 shows that these are 12% and 20%, respectively. The coupled TG-MS analysis reveals that the evolved gases are oxygen (O_2 , $m/z=32$) and steam (H_2O , $m/z=18$). The red curve assigned to O_2 has a small first peak and a large second peak. The blue curve assigned to H_2O is related to the crystal structure. Comparing the theoretical weight loss of the proposed reactions (columns 2 and 3 in Table 2) with the experimental results demonstrates the simultaneous desorption of O_2 and H_2O from $\text{CoO}(\text{OH})$ into Co_3O_4 at around 280 °C.

The second weight loss, confirmed by MS analysis, shows the decomposition of Co_3O_4 to CoO at around 850 °C. Therefore, the

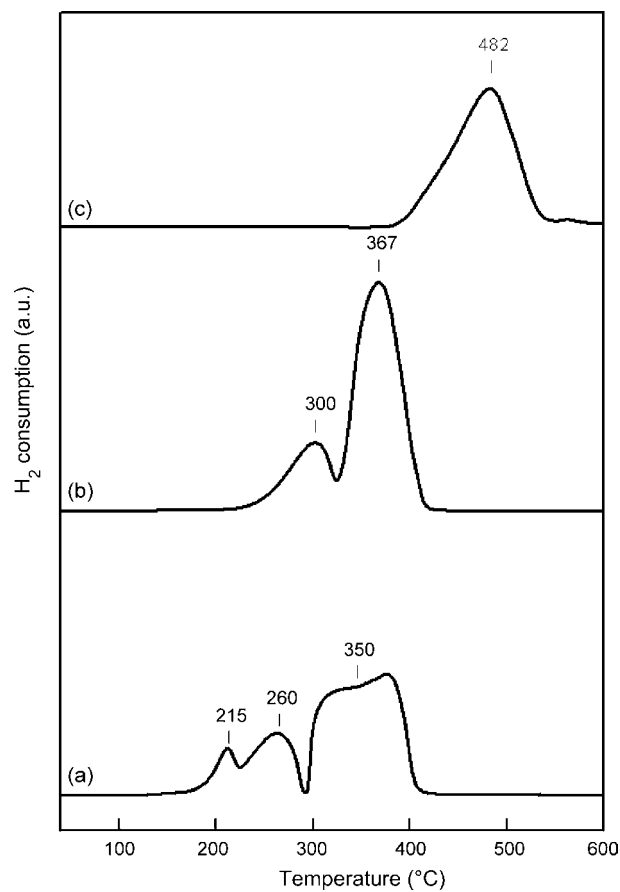


Fig. 5. TPR profiles of (a) D-280 (b) D-450 (c) D-950.

D-280 sample can be decomposed into Co_3O_4 and then CoO under heat treatment.

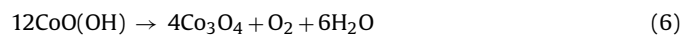


Fig. 7 shows the TG-MS profile of the D-450 sample. At under 300 °C, the tardy weight loss is associated with desorption of adsorbed water on the surface of Co_3O_4 . The red curve is assigned

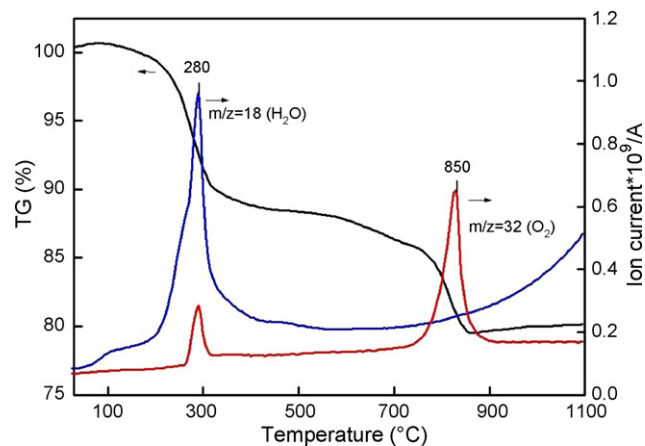


Fig. 6. Analysis of the outlet gases from the decomposition of D-280 by TG-MS (heating rate of $10^\circ\text{C min}^{-1}$ under He): H_2O (blue) and O_2 (red). (For interpretation of the references to color in this figure legend, the reader is referred to the web version of the article.)

Table 2
Experimental and theorization of a series of cobalt oxide for TG-MS

Sample	Reaction process	Weight loss (%) ^a		Outlet gas (C) ^b	
		Theoretical	Experimental	H ₂ O	O ₂
CoOOH ^c	12CoO(OH) → 4Co ₃ O ₄ + O ₂ + 6H ₂ O	13	12	300	920
	2Co ₃ O ₄ → 6CoO + O ₂	19	20		
Co ₃ O ₄ ^c	2Co ₃ O ₄ → 6CoO + O ₂	7	8	–	820
CoO ^d	6CoO + O ₂ \xrightarrow{A} 2Co ₃ O ₄ \xrightarrow{B} 6CoO + O ₂	A:7 B:-7	A:7 B:-8	–	920

^a Measurement of TG.

^b Measurement of mass analyzer.

^c By TG-MS flow He.

^d By TG-MS flow air.

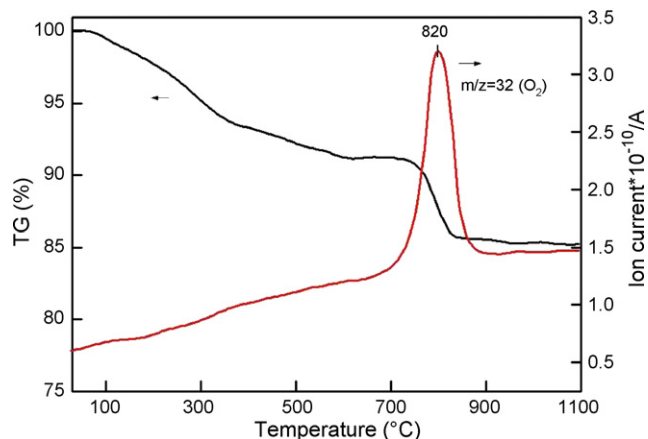


Fig. 7. Analysis of the outlet gases from the decomposition of D-450 by TG-MS (heating rate of 10 °C min⁻¹ under He): O₂ (red). (For interpretation of the references to color in this figure legend, the reader is referred to the web version of the article.)

to O₂ at 820 °C. The weight loss of 8% is caused mainly by the decomposition of Co₃O₄ to CoO, according to Eq. (7).

Fig. 8 shows the TG profile of the D-950 sample in air. The weight increase of 7% involves mainly the oxidation of CoO to Co₃O₄ as the temperature is increased from 250 to 900 °C, followed by the desorption of oxygen to CoO at above 900 °C. Comparing the theoretical weight variations of the proposed reaction (columns 2 and 3 in Table 2) with the experimental results demonstrated that CoO can undergo oxidation–reduction in air, according to Eq. (8).

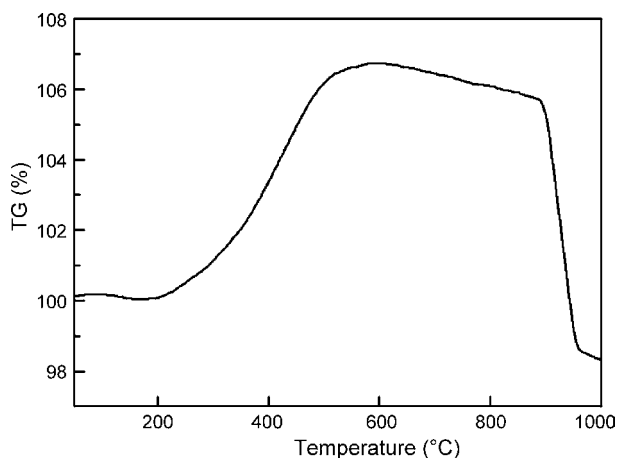
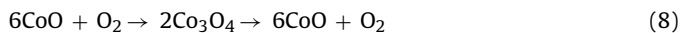


Fig. 8. TG profile of D-950 at a heating rate of 10 °C min⁻¹ under air.

4. Conclusions

A convenient procedure for preparing a series of pure cobalt oxides is presented; it involves the decomposition of CoO_x in a nitrogen environment at different temperatures.

TG-MS, XRD, Raman, FTIR and TPR analyses are demonstrated to be useful in identifying the series of cobalt oxides. The D-280 sample [CoO(OH)] has a hexagonal structure that gives rise to Co₃O₄ and CoO in helium at 280 and 850 °C, respectively. The D-450 sample [Co₃O₄] has a spinel structure that gives rise to CoO in helium at 820 °C. The D-950 sample [CoO] has a faced-centered cubic structure that can be oxidized to Co₃O₄ at 200–600 °C and decomposed to CoO at 850–1000 °C in air, respectively. The preparation of materials and the analysis of their thermal behavior is a convenient way to control and determining the purity of cobalt oxide.

Acknowledgements

We are pleased to acknowledge financial supports for this study from Academia Sinica and the National Science Council of the Republic of China.

References

- [1] F. Lichtenberg, K. Kleinsorgen, J. Power Sources 62 (1996) 207.
- [2] H.K. Lin, H.C. Chiu, H.C. Tsai, S.H. Chien, C.B. Wang, Catal. Lett. 88 (2003) 169.
- [3] S.A. Makhlof, J. Magn. Mater. 246 (2002) 184.
- [4] H. Yamaura, K. Moriya, N. Miura, N. Yamazoe, Sens. Actuators B 65 (2000) 39.
- [5] R. Van Zee, Y. Hamrick, S. Li, W. Weltner, J. Phys. Chem. 96 (1992) 7247.
- [6] Comprehensive Inorganic Chemistry, vol. 3, Pergamon Press, Oxford, 1973, p. 1107.
- [7] M. Elemony, M. Gouda, Y. Elewady, J. Electroanal. Chem. 76 (3) (1977) 367.
- [8] D. Chen Yih-Wen, N.N. Rommel, J. Electrochem. Soc. 131 (4) (1984) 731.
- [9] C.B. Wang, H.K. Lin, C.W. Tang, Catal. Lett. 94 (2004) 69.
- [10] A. Berger, M.J. Pechan, R. Compton, J.S. Jiang, J.E. Pearson, S.D. Bader, Phys. Rev. B 306 (2001) 235.
- [11] M. Rubinstein, P. Lubitz, S.F. Cheng, J. Magn. Mater. 195 (1999) 299.
- [12] N. Koshizaki, K. Yasumoto, T. Sasaki, Nanostruct. Mater. 12 (1999) 971.
- [13] N. Koshizaki, K. Yasumoto, T. Sasaki, Sens. Actuators B 66 (2000) 122.
- [14] G.A. El-Shobaky, T. El-Nabarawy, I.F. Hewaidy, Surf. Technol. 10 (1980) 225.
- [15] G.A. El-Shobaky, I.F. Hewaidy, N.M. Ghoneim, Thermochim. Acta 53 (1982) 105.
- [16] G.A. El-Shobaky, T. El-Nabarawy, T.M. Ghazy, Surf. Technol. 15 (1982) 153.
- [17] L. Börnstein, Physics of Non-tetrahedrally Bonded Binary Compounds, 17, Springer, New York, 1984.
- [18] C. Wanger, E. Kock, Z. Phys. Chem. B 31 (1936) 439.
- [19] P. Kostad, Non-stoichiometry, in: Diffusion and Electrical Conductivity in Binary Metal Oxides, Wiley-Interscience, New York, 1972, p. 426.
- [20] G.A. El-Shobaky, T. El-Nabarawy, I.F. Hewaidy, Surf. Technol. 10 (1980) 311.
- [21] M. Figlarz, J. Guenot, F. Fievent-Vincent, J. Mater. Sci. 11 (1976) 2267.
- [22] S.G. Christoskova, M. Stoyanova, M. Georgieva, D. Mehandjiev, Mater. Chem. Phys. 60 (1999) 39.
- [23] T. Andrushkevich, G. Boreskov, V. Popovskii, L. Pliasova, L. Karakchiev, A. Ostantkovitch, Kinet. Catal. 6 (1968) 1244.
- [24] Y. Okamoto, H. Nakano, T. Imanaka, S. Teranishi, Bull. Chem. Soc. Jpn. 48 (1975) 1163.
- [25] C. Spenser, D. Schroeder, Phys. Rev. B 9 (1974) 3658.
- [26] J. Llorca, P.R. Piscina, J.A. Dalmon, N. Homs, Chem. Mater. 16 (2004) 3573.

- [27] V.G. Hadjiev, M.N. Iliev, I.V. Vergilov, *J. Phys. C: Solid State Phys.* 21 (1988) L199.
- [28] H.C. Choi, Y.M. Jung, I. Noda, S.B. Kim, *J. Phys. Chem. B* 107 (2003) 5806.
- [29] M.M. Vuurman, D.J. Stufkens, A. Oskam, G. Deo, I.E. Wachs, *J. Chem. Soc., Faraday Trans. 92* (1996) 3259.
- [30] C.A. Melendres, S.J. Xu, *J. Electrochem. Soc.* 131 (1984) 2239.
- [31] B.A. Sexton, A.E. Hughes, T.W. Turney, *J. Catal.* 97 (1986) 390.
- [32] H.Y. Lin, Y.W. Chen, *Mater. Chem. Phys.* 85 (2004) 171.
- [33] C.B. Wang, C.W. Tang, S.J. Gau, S.H. Chien, *Catal. Lett.* 101 (2005) 59.
- [34] P. Arnoldy, J.A. Moulijn, *J. Catal.* 93 (1985) 38.
- [35] M. Vob, D. Borgmann, G. Wedler, *J. Catal.* 212 (2002) 10.